# Direct Membrane Retrieval into Large Vesicles After Exocytosis in Sea Urchin Eggs

**Tim Whalley,* Mark Terasaki,‡ Myoung-Soon Cho,* and Steven S. Vogel***

*Laboratory of Theoretical and Physical Biology, National Institute of Child Health and Human Development; and ‡Laboratory of Neurobiology, National Institute of Neurological Disorders and Stroke, National Institutes of Health, Bethesda, Maryland 20892

***Abstract.*** At fertilization in sea urchin eggs, elevated cytosolic $Ca^{2+}$ leads to the exocytosis of 15,000–18,000 1.3-μm-diam cortical secretory granules to form the fertilization envelope. Cortical granule exocytosis more than doubles the surface area of the egg. It is thought that much of the added membrane is retrieved by subsequent endocytosis. We have investigated how this is achieved by activating eggs in the presence of aqueous- and lipid-phase fluorescent dyes. We find rapid endocytosis of membrane into 1.5-μm-diam vesicles starting immediately after cortical granule exocytosis and persisting over the following 15 min. The magnitude of this membrane retrieval can compensate for the changes in the plasma membrane of the egg caused by exocytosis. This membrane retrieval is not stimulated by PMA treatment which activates the endocytosis of clathrin-coated vesicles. When eggs are treated with short wavelength ultraviolet light, cortical granule exocytosis still occurs. but granule cores fail to disperse. After egg activation, large vesicles containing semi-intact cortical granule protein cores are observed. These data together with experiments using sequential pulses of fluid-phase markers support the hypothesis that the bulk of membrane retrieval immediately after cortical granule exocytosis is achieved through direct retrieval into large endocytotic structures.

In many cells a burst of exocytotic activity is followed by a burst of endocytotic activity (24, 29, 38, 40); this has led to the idea that these two processes are coupled in some way to maintain cell surface area. One way to couple these two processes and maintain membrane surface area after secretion would be to internalize endocytotic structures of a number and size similar to the vesicles that fused with the plasma membrane during exocytosis. Consistent with this, in chromaffin cells (4), posterior pituitary nerve endings (39), and in melanotrophs (52), endocytotic vesicles that are as large as, or larger than the corresponding secretory vesicles have been shown to form after triggered exocytosis. It is unclear how cells with large exocytotic granules would maintain cell surface area via a mechanism involving receptor-mediated endocytosis of small clathrin-coated vesicles (47). Perhaps exocytotic vesicles fuse with the plasma membrane and reseal after release of their contents. The phenomenon of "flicker-fusion" illustrates that exocytotic vesicles can transiently fuse with plasma membranes (3, 7, 19, 58). Alternatively, endocytotic vesicles of similar size to the exocytotic vesicles might be formed de novo after secretion by the direct retrieval of plasma membrane. Teleologically, there are benefits in each retrieval route. In the first, retrieval is simple and secretory vesicle membrane insertion is merely a means of delivering the vesicular contents to the exterior of the cell. In this scheme, the same proteins that mediate vesicle fusion may also mediate endocytosis. Maintenance of cell surface area is achieved by closing the fusion pore, thus retrieving the same number and size vesicles that fused with the plasma membrane. In the latter pathway, additional cellular components such as clathrin (28, 53) or dynamin (11, 41, 43) might be necessary to mediate membrane retrieval. This mechanism may allow extensive sorting of plasma membrane lipids and proteins that might be important for regulating cellular activity.

The elevation of the fertilization envelope during sea urchin egg activation is a consequence of the coordinated exocytosis of thousands of 1.3-μm-diam cortical secretory granules (in *Strongylocentrotus purpuratus*) (46) and is triggered by the release of $Ca^{2+}$ from intracellular stores (15). Exocytosis more than doubles the surface area of the egg (26, 34, 46). Unfertilized sea urchin egg plasma membranes appear to possess clathrin plaques (45), and the rapid formation of coated pits and vesicles after fertilization or egg activation has been demonstrated using electron microscopy (9, 20, 21). However, it is thought that this clathrin-dependent endocytosis is independent of cortical granule exocytosis, and its magnitude has not been quanti-

Address all correspondence to Dr. S. S. Vogel, Building 10 Room 10D09, National Institutes of Health, Bethesda, MD 20892. Tel.: (301) 594-2658. Fax: (301) 594-0813.

T. Whalley's present address is Department of Biological and Molecular Sciences, University of Stirling, Stirling, FK9 4LA, Scotland, UK. M. Teraski's present address is Department of Physiology, University of Connecticut Health Center, Farmington, CT 06032.

tated (20, 21). It has remained unclear how the egg compensates for the increase in plasma membrane area after cortical granule exocytosis. In this study we have used confocal microscopy, electron microscopy, and a fluorimetric assay to determine whether endocytosis through the classic coated vesicle pathway is the sole means of membrane retrieval after sea urchin egg activation or whether other membrane retrieval pathways are operable.

## Materials and Methods

### Obtaining and Handling Gametes

Eggs and sperm of the sea urchin *Strongylocentrotus purpuratus* or *Lytechinus variegatus* were obtained by intracoelomic injection of 0.5 M KCl. Eggs were collected in artificial sea water (ASW[1]; 435 mM NaCl, 40 mM $MgCl_2$, 15 mM $MgSO_4$, 11 mM $CaCl_2$, 10 mM KCl, 10 mM Hepes, 1 mM EDTA, pH 8.0) and sperm were collected dry. Before fertilization, eggs were dejellied by several passes through 90- or 110-μm Nitex mesh (Tetko Inc., Elmsford, NY) and were washed three times in ASW. Batches of eggs exhibiting <98% fertilization were rejected.

### Confocal Microscopy

For confocal microscopy eggs were attached to polylysine-treated glass coverslips and mounted in a microscope perfusion chamber. For fertilization, eggs were perfused with ASW containing a 1:1,000 dilution of sperm. An MRC 600 (Bio-Rad Laboratories, Hercules, CA) with a krypton-argon laser coupled to an Axioscope (Carl Zeiss, Inc., Thornwood, NY) was used for microscopy (50). A Plan-apo ×63 NA 1.4 lens was used. The 488- and 568-nm lines of a krypton-argon laser and the standard filters (K1 and K2; Bio-Rad Laboratories) were used for simultaneous dual fluorescence imaging. The video signal from the confocal scan card was passed through a time-date generator (WJ 810; Panasonic, Secaucus, NJ) and recorded on an optical recorder (3031F; Panasonic). The microscope was set to scan continuously at either the normal or fast rate. The speed of the scan rate was determined by using a stop watch to scan 100 frames; the normal scan rate was 1.07 s/frame and the fast rate was 0.535 s/frame. To record the images, the record button on the optical recorder was pressed manually as the scan reached the bottom of the monitor.

### Quantitating Membrane Retrieval After Egg Activation

For all experiments, 5% suspensions of eggs were used. Sperm were diluted 1:100 in ASW immediately before use and fertilization was achieved by mixing eggs and diluted sperm at a volume ratio of 50:1. When eggs were activated by A23187, this was dissolved in DMSO and was added to give a final concentration of 50 μM. Dye-uptake experiments were performed in 2.5-cm-diam plastic dishes. Tetramethylrhodamine-dextran (Rh-dex; mol wt 3,000; Molecular Probes, Eugene, OR) was dissolved in ASW. It was used at a final concentration of ~100 μM and was added to the eggs 15 min before the start of an experiment. Rh-dex that was passed over a 10-ml Sephadex G25 (Sigma Chemical Co., St. Louis, MO) column to ensure the removal of free tetramethylrhodamine gave essentially the same results as nonchromatographed Rh-dex. After activation, 0.5-ml aliquots of eggs were taken at intervals and dye uptake arrested by dilution into 15 ml of ice-cold calcium-free buffer (PKME; 50 mM Pipes, 450 mM KCl, 10 mM $MgCl_2$, 5 mM EGTA, pH 6.7). Eggs were pelleted by centrifugation at 300 *g* for 30 s at 4°C, the supernatant was aspirated and the pellet resuspended in 10 ml ice-cold PKME. This was repeated twice more. After the final aspiration, the pellet was resuspended in 1 ml 2.5% Triton X-100 and dispersed using a sonicator (Branson Ultrasonics Corp., Danbury, CT). Rh-dex uptake was determined using a microtiter plate reader (Fluoroskan II; Labsystems, Helsinki, Finland) using an excitation wavelength of 544 nm (band width 15 ± 2 nm) and an emission wavelength of 590 nm (band width 14 ± 2 nm). Background dye associated with nonactivated eggs was always subtracted to give a value for stimulated dye internalization. There was no significant difference in the amount of background dye associated with eggs during 1-, 2-, 2.5-, or 17.5-min pulses as determined by analysis of variance (F-Ratio = 0.402, Degrees of freedom = 3,12). Protein concentration was determined using a BCA protein assay kit (Pierce Chemical Co., Rockford, IL).

### UV Treatment of Eggs

1-ml vols of 5% suspensions of eggs in 3-cm-diam plastic petri dishes were treated with UV light with a wavelength of 254 nm using a hand-held UV lamp (UVP Inc., Upland, CA) at a distance of 2 cm with agitation every 30 s. 100 μM Rh-Dex was added to the eggs which were then activated by the addition of 50 μM A23187 and dye uptake determined as above, or the eggs were fixed for electron microscopy.

### Electron Microscopy

Eggs were washed with ASW and fixed with ASW containing 3% glutaraldehyde for 1 h at 22°C and overnight at 4°C. The eggs were washed in Hendry's phosphate buffer and were postfixed in 1% $OsO_4$ in the same buffer. The eggs were then washed in distilled water and stained with saturated uranyl acetate for 15 min. Samples were dehydrated in a graded ethanol and acetone series. Dehydrated samples were embedded in Epon-Araldite and cured at 60°C for 48 h. Cured blocks were ultrathin sectioned using an Ultratome V (LKB Instruments, Inc., Bromma, Sweden). Sections were stained with saturated uranyl acetate and Reynold's lead citrate and were observed in a transmission electron microscope (CM10; Philips Technologies, Cheshire, CT).

## Results

Underlying the plasma membrane of an unfertilized egg is a population of vesicles with a distinct electron dense lamellar morphology most striking in *S. purpuratus* (Fig. 1 *A*). These are the cortical secretory vesicles or cortical granules and their lamellar morphology is due to the tight packing of the protein contents. During egg activation these granules fuse with the plasma membrane, their contents are released, and the expansion of the extruded granule cores leads to the elevation of the fertilization membrane. After fertilization, the cortical granules are no longer observed by electron microscopy and appear to be replaced by a population of clear vesicles (Fig. 1 *B*). The origin of these vesicles is unknown.

### Confocal Imaging of Membrane Retrieval

We attempted to visualize endocytosis at fertilization in sea urchin eggs by using the fluorescent aqueous marker Rh-dex, and the fluorescent membrane markers RH 414 and FM 1-43. These markers are all membrane impermeant. We used confocal microscopy to visualize the cortical regions of eggs bathed in sea water containing Rh-dex (100 μM). Before fertilization we found little detectable endocytotic activity as judged by the formation of fluorescent inclusions in the egg cytoplasm during a 15-min incubation (Fig. 2 *A*). Typically ~30 s after the addition of sperm, a wave of punctate fluorescence rapidly traversed the cortical region of the egg emanating from the point of sperm–egg interaction (Fig. 2 *B*). Since the fluorescent spots indicated by the arrows in Fig. 2 *C* were not evident in the previous image (1 s previous) (Fig. 2 *B*), the formation of these structures is very rapid. The initial appearance of these spots corresponds to exocytosis (50; also see below). Subsequent removal of extracellular Rh-dex by washing with dye-free ASW indicated that a subpopulation of the fluorescent structures were internal and had no

1. *Abbreviations used in this paper*: ASW, artificial sea water; DIC, differential interference contrast; Fl-dex, fluorescein-conjugated dextran; Rh-dex, tetramethylrhodamine-conjugated dextran.

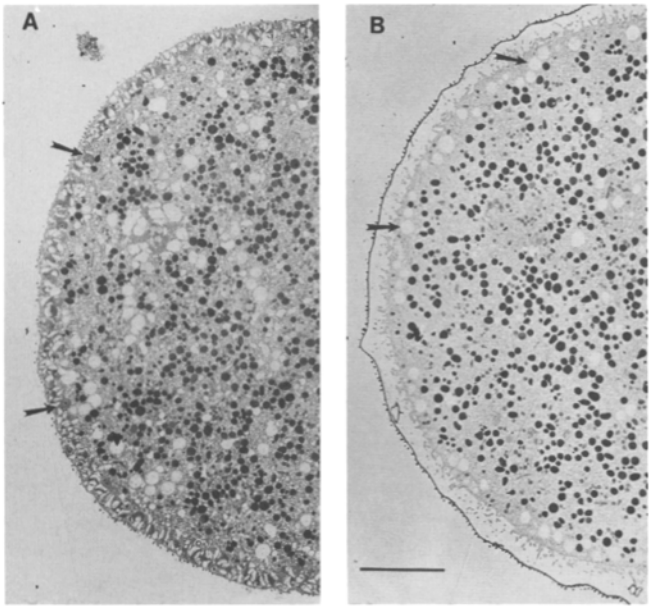


*Figure 1.* Electron micrographs of an unfertilized and fertilized egg. (*A*) A section through the cortex of an unfertilized egg. The structures indicated with the arrows are cortical secretory granules and their protein contents give rise to their characteristic lamellar morphology. (*B*) A section through the cortex of an egg 5 min after fertilization. The cortical granules are no longer present. The release of the granule contents has led to the formation of the fertilization envelope. Indicated with the arrows are clear vesicles which are now present in the egg cortex. Bar, 10 μm.

extracellular continuity (Fig. 2 *D*). These fluorescent structures had a mean diameter of 1.5 ± 0.1 μm (mean ± SEM, $n = 54$), and ranged in size from 0.2 to 2.9 μm. The origin of this size distribution is not known, but it may represent some fundamental variability inherent in the mechanism of their formation.

We also used RH-414, another marker that has been particularly useful for detecting endocytosis (5, 44). RH-414 is soluble in both water and membranes, but has a low fluorescence in water. When partitioned into membranes, it exhibits a dramatic increase in fluorescence. Confocal microscopic images of three eggs bathed in ASW containing 1 μM RH-414 are shown in Fig. 3 *A*. The ASW surrounding the eggs is not fluorescent; bright fluorescence is only seen in the plasma membranes of the eggs. Little endocytotic activity was detected before fertilization. As with Rh-dex, there was a wave of fluorescent labeling that passed across the egg surface at fertilization and greatly increased the membrane fluorescence (Fig. 3 *B*). Similar ringlike labeling was previously observed with the related dye FM 1-43 (50). To demonstrate that the initial fluorescent membrane labeling is due to exocytosis, we simultaneously imaged the cortical granules by differential inter-

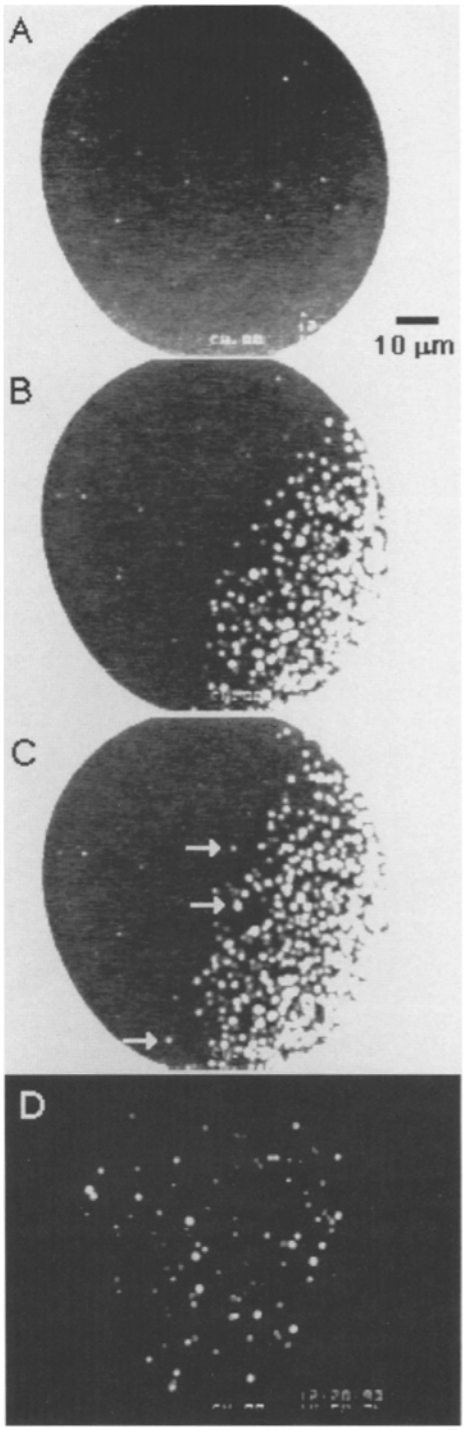


*Figure 2.* Subcortical localization of Rh-dex during sea urchin cortical granule exocytosis. Subcortical confocal optical sections of a sea urchin egg were captured to study plasma membrane events during egg fertilization. (*A*) An unfertilized sea urchin egg in ASW containing 100 μM Rh-dex (3,000 mol wt). The egg has been pretreated for 1 min with ASW containing 100 μM amino-dextran (3,000 mol wt) to decrease nonspecific binding of our fluorescent probe. Note the fluorescence all around the egg but occluded from the cytoplasm by the egg's plasma membrane. (*B*) 24 s after adding sperm (1:1,000 dilution in ASW; at t = 0 s) we see a wave of formation of punctate fluorescent bodies. In this egg, the appearance of these bodies crossed the subcortical region of the egg from the lower right toward the upper left quadrant. (*C*) Within 1 s (at t = 25 s) we see the formation of new punctate bodies (*arrows*). The egg was washed at t = 30 s with ASW to remove extracellular Rh-dex. (*D*) At t = 105 s we see large fluorescent inclusions in the subcortical region of the fertilized egg. Note that the extracellular fluorescence seen in *A*, *B*, and *C* and many of the fluorescent bodies observed in *B* and *C* are no longer observed.

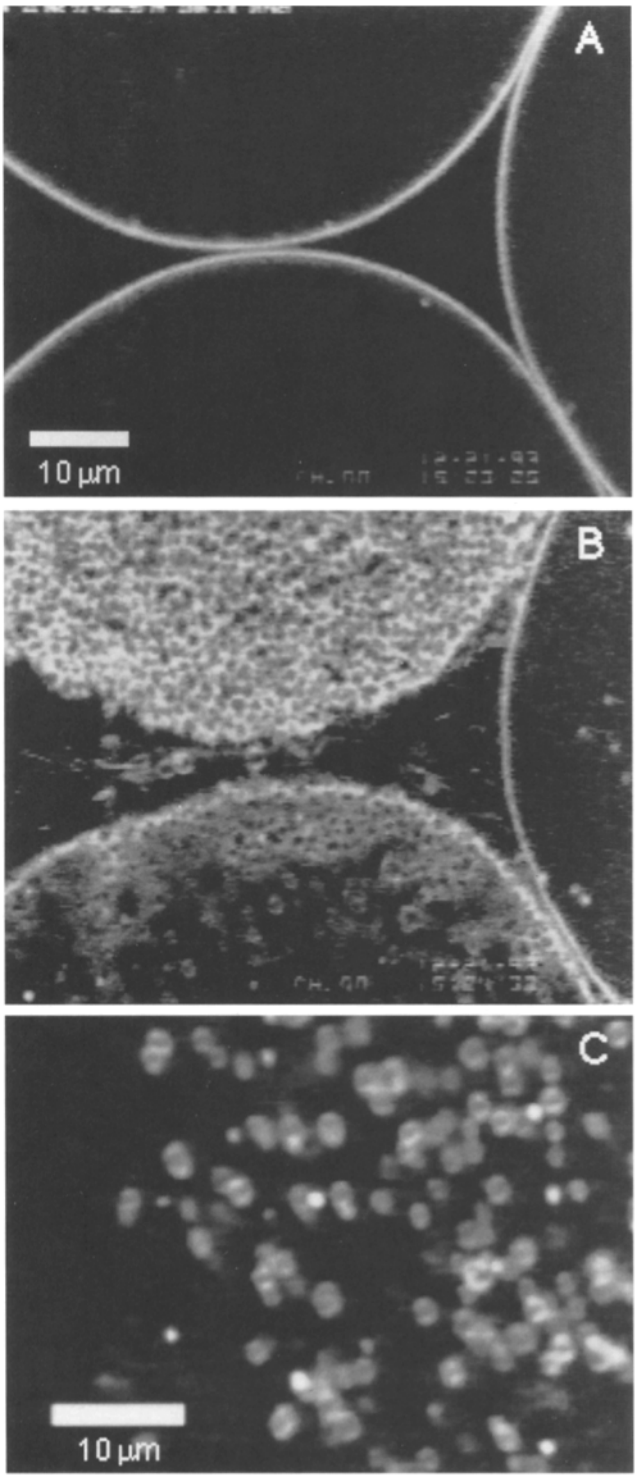


*Figure 3.* Subcortical localization of the fluorescent membrane probe RH-414 during sea urchin cortical granule exocytosis. (*A*) A subcortical optical section of three eggs in ASW containing 1 μM RH-414. Note that RH-414 fluorescence is only observed in the plasma membrane and is not observed in the surrounding sea water or in intracellular membranes. (*B*) After adding sperm we now see fluorescent bodies in the surrounding sea water which are the RH-414–labeled membranes of the added sperm. We also see a dramatic increase of fluorescence in the cortical region of the eggs when they are fertilized. The top egg was the first to be fertilized, the bottom egg is in the midst of being fertilized, and the egg at the left has not yet been fertilized. Eggs were washed with ASW 2 min after adding sperm to remove RH-414 from the surrounding sea water and from the contacting egg plasma membrane. At a higher magnification we observe ringlike fluorescent labeling in the subcortical region of fertilized eggs which remain after the wash while the plasma membrane (at the left of the field) is not fluorescent (*C*).

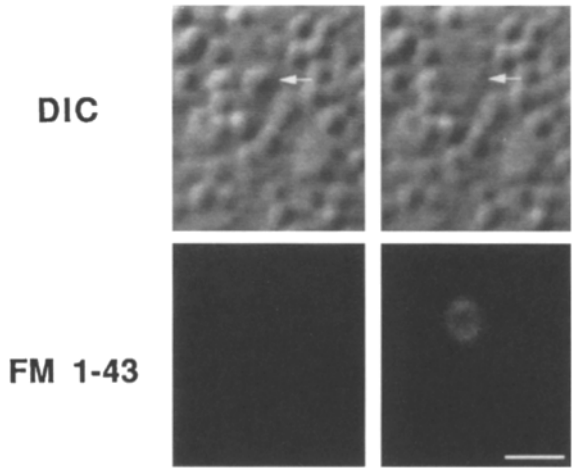


*Figure 4.* Correlation of cortical granule fusion with the appearance of FM 1-43 fluorescence. A region of the cortex of an egg was visualized simultaneously using scanning DIC (*top row*) and FM 1-43 fluorescence (*bottom row*) during egg activation. The appearance of the FM 1-43–labeled ring corresponded with the disappearance of the cortical granule at the same location (*white arrows*). The images were obtained 0.535 s apart. Bar, 2.5 μm.

ference contrast (DIC) and appearance of fluorescent structures after fertilization of eggs bathed with 2 μM FM 1-43 (Fig. 4). The dispersal of the cortical granule contents (*white arrow*) is directly correlated with the appearance of a fluorescent ring. Interestingly, the diameter of the fluorescent ring appears slightly larger than the diameter of the DIC granule image. We perfused eggs with ASW to remove exogenous dye 1 min after the addition of sperm. Plasma membrane–associated fluorescence was effectively removed, but many ringlike fluorescent structures were still visible (Fig. 3 *C*) indicating that they were no longer continuous with the extracellular medium and thus at this point represented endocytotic structures.

We determined that both the aqueous and lipid markers were labeling identical structures by incubating fertilizing eggs in ASW containing both Rh-dex and FM 1-43, a membrane marker that has physical properties very similar to those of RH-414, but with fluorescence spectral properties more similar to fluorescein. This dual labeling with aqueous and lipid markers should label the lumen and membrane of the same structures. 2 min after fertilization, many structures had been formed consisting of red circles (the aqueous marker Rh-dex) surrounded by a yellow ring (caused by the overlap of the green membrane marker FM 1-43 and the red fluid-phase marker) (Fig. 5). These intracellular structures are therefore membrane vesicles with aqueous contents that once mixed with the extracellular milieu.

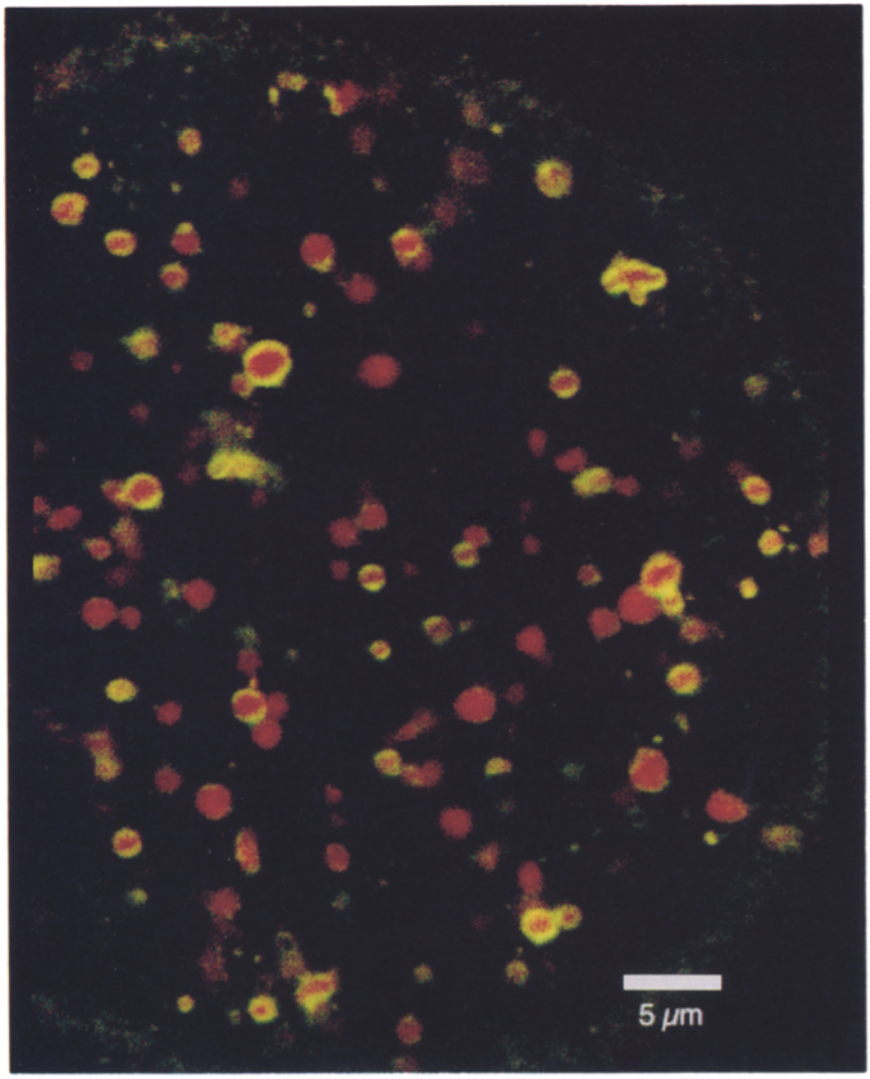


*Figure 5.* Colocalization of the fluid-phase marker Rh-dex and the membrane marker FM 1-43 in large subcortical intracellular vesicles. Sea urchin eggs were fertilized in ASW containing 100 μM Rh-dex (3,000 mol wt) and 1 μM FM 1-43. After 2 min, the eggs were washed with ASW and a confocal optical section of the subcortical region was captured on two channels of a confocal microscope (using rhodamine and fluorescein optics) revealing large red fluorescent bodies (Rh-dex) surrounded by yellow fluorescent membranes (FM 1-43).

### *Time Course and Magnitude of Membrane Retrieval*

To characterize the time course and extent of membrane retrieval after egg activation, we developed an assay for measuring fluorescent dextran uptake in populations of eggs. Eggs were incubated in Rh-dex–containing ASW, fertilized or activated using the $Ca^{2+}$-ionophore A23187, and dye uptake arrested by adding the eggs to ice-cold calcium-free buffer. The egg-associated fluorescence and protein concentration were determined to calculate the volume of marker internalized. We detected no increase in dye uptake over a 15-min period in unfertilized eggs (data not shown), consistent with our observations using confocal microscopy (see Fig. 2 *A*). Dye uptake was detected 30 seconds after the addition of sperm and continued over the following 15 min (Fig. 6 *A*). The half-time for dye uptake was ~5 min. We found that activation by the calcium ionophore A23187 gave very similar results to fertilization, suggesting that uptake was triggered by elevated levels of intracellular $Ca^{2+}$ (Fig. 6 *A*). The finding that the amount of Rh-dex internalized was linear when used at 25–250 μM (data not shown), and that inclusion of nonlabeled aminodextran did not reduce the amount of fluorescent dextran internalized (data not shown), argue that Rh-dex within this concentration range is a fluid-phase marker and that dextran binding to a saturatable receptor is not a requirement for uptake. Ultimately a net value of ~6% of an egg's starting volume was internalized. This value is ~65% of the volume of a 1.3-μm-thick shell of the 80-μm-diam eggs cortical region, and can compensate for the volume lost to the egg when 14,000 cortical granules fuse. To characterize the rate of retrieval we measured uptake during eight consecutive pulses of extracellular dye (each pulse lasting 1–2.5 min) for 17.5 min after egg activation. This indicated that the rate of dextran uptake was maximal between three and five minutes after activation (Fig. 6 *B*). We compared the amount of dye retained by activated eggs in response to one 17.5-min pulse, which was 6.2 ± 1.1% (mean ± SD; $n = 4$) of the cell volume compared with 8.0 ± 1.9% (mean ± SD; n = 4) of the cell volume as measured by the summation of the eight individual pulses. A conservative estimate of the probability that these two values are not drawn from the same underlying distributions is between 90 and 95% (Student's *t* test). It is therefore unclear if the difference in the amount of dye uptake observed by these two protocols is a statistical fluctuation, or due to an underlying biological process such as dye release via direct fusion, transport, and release of dye via

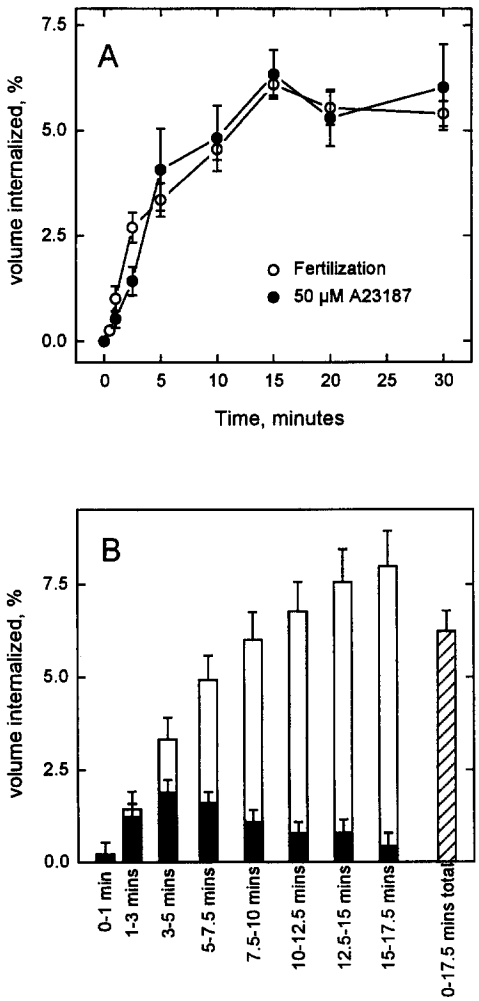


*Figure 6.* Time course and extent of membrane retrieval after egg activation. Sea urchin gametes were collected as described and Rh-dex uptake determined at various times after activation. (*A*) When eggs were activated by fertilization or by the addition of 50 μM A23187, dye uptake was detected within 30 s and continued over the next 15 min. Fertilization or treatment with the $Ca^{2+}$ ionophore A23187 stimulated uptake to the same extent. Mean ± SEM are shown, $n = 5$. (*B*) We used pulses of Rh-dex to further characterize the extent of membrane retrieval after activation by A23187. We measured dye uptake during eight consecutive pulses of extracellular dye (*black bars*; each pulse lasting 1–2.5 min and eggs were immediately quenched on ice after the pulse) for 17.5 min. White bars indicate the cumulative sum of the black bars. We also measured dye uptake in response to one 17.5 min pulse (*striped bar*). Mean ± SEM are shown, $n = 4$.

small vesicular carriers, or simply due to intracellular dye degradation.

### *Direct Formation of Large Endosomes*

Only a subset of the structures visible in Fig. 2 *C* is present in Fig. 2 *D*, indicating that most of the structures observed in Fig. 2 *C* were large invaginations of the plasma membrane that are continuous with the extracellular milieu. What is unclear is whether the structures that have pinched off the plasma membrane are derived from these large invaginations, or are they formed via a concomitant mechanism where small clathrin-coated vesicles pinched off from the plasma membrane and fused together inside the fertilized egg. We tested which of these mechanisms was operating by performing sequential labeling experiments. 1 min after fertilization, we perfused eggs with fluorescein-conjugated dextran (Fl-dex) ASW and incubated for 30 s. After a 1-min wash we perfused the eggs with Rh-dex ASW and incubated for 30 s. Finally, we washed the eggs with dye-free ASW and determined the intracellular location of each marker. Virtually all of the vesicles appeared either red or green indicating that the two markers are located in different intracellular compartments dispersed among each other throughout the field (Fig. 7). Occasionally a region of a vesicle appeared yellow, probably due to optical overlap of Fl-dex– and Rh-dex–containing vesicles. Alternatively, yellow vesicles might represent infrequent lateral fusion. When eggs were fertilized in ASW containing both dyes we observed that all of the internalized structures contained both markers (data not shown). If we were labeling preexisting structures such as endosomes by the fusion of many small clathrin-coated vesicles we would expect substantial colocalization of dyes in this experiment. Our failure to observe this suggests that the fluorescent structures form at this size as the direct result of membrane retrieval subsequent to exocytosis and not through the fusion of many small clathrin-coated vesicles.

If the large endosomes observed after egg activation are formed by the direct retrieval of surface membrane into large endosomes it might be possible to ensnare large structures in the lumina of these endosomes. This would be impossible if these endosomes were formed from the fusion of multiple small coated vesicles. We took advantage of the unique morphology of *S. purpuratus* cortical granule contents to investigate this possibility. Illuminating unfertilized eggs with short wavelength (~254 nm) UV light inhibits the elevation of the fertilization envelope (48). Eggs were treated with 254 nm UV light after which fertilization envelope elevation and Rh-dex uptake in response to 50 μM A23187 were determined. Over a 15-min treatment period, fertilization envelope elevation was progressively inhibited. Surprisingly, Rh-dex uptake appeared to be unaffected (Fig. 8). There was no significant difference between the level of endocytosis in eggs with a full fertilization envelope and those with none. We used electron microscopy to determine precisely what effect UV treatment was having on cortical granule exocytosis. The morphology of unfertilized UV-treated eggs (Fig. 9 *A*) was indistinguishable from nontreated unfertilized eggs (Fig 1 *A*). The cortical granules retained their characteristic lamellar structure and were tightly associated with the plasma membrane. After activation the effect of UV treatment became apparent. Whereas in non-UV–irradiated, A23187-activated eggs the cortical granule contents have disappeared, in UV-irradiated eggs the cortical granule contents were still visible after activation. Apparently UV treatment does not arrest membrane fusion but prevents the expansion of the protein contents of the cortical granules and thus arrests the elevation of the fertilization envelope. Lamellar contents were observed between the plasma membrane and the vitelline membrane arguing that membrane fusion was not inhibited. Cortical granule contents were also observed to be trapped in the lumina of the large otherwise transparent subcortical vesicles (Fig. 9 *B*).

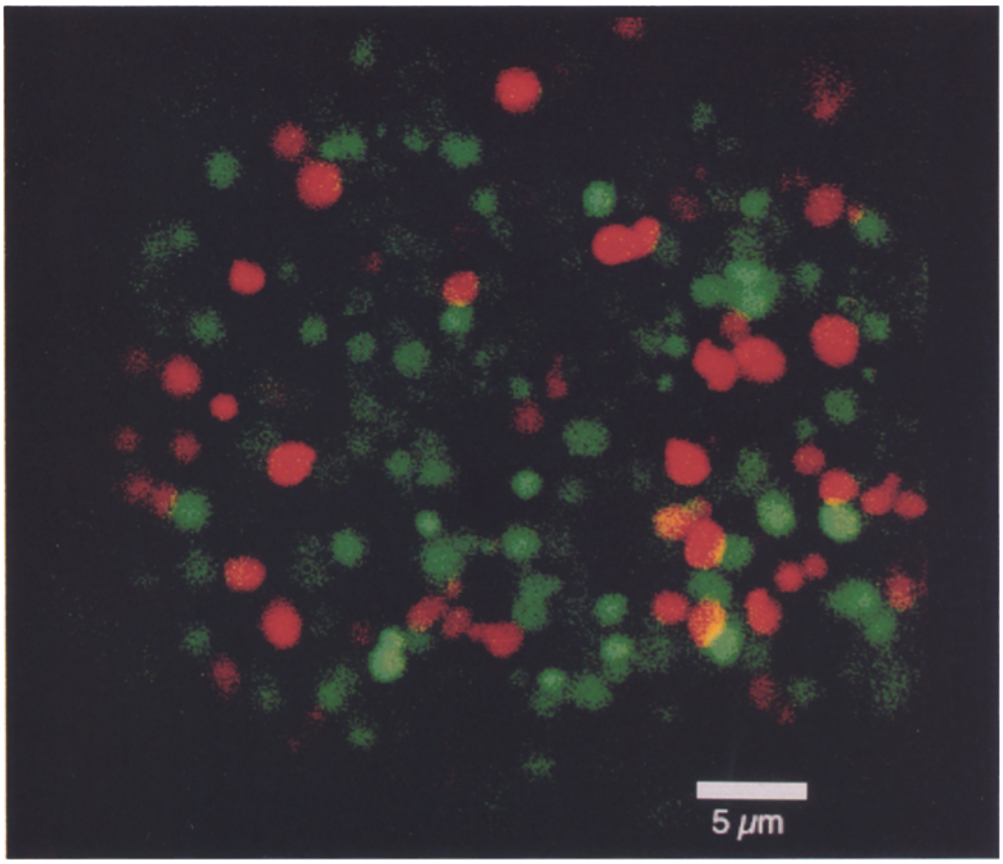


*Figure 7.* Evidence that large endocytotic vesicles are formed by the direct retrieval of surface membranes. Sperm was added to eggs for 1 min and then incubated in ASW containing 100 μM Fl-dex (3,000 mol wt) for 30 s. Next the eggs were washed for 1 min in ASW and then incubated in ASW containing 100 μM Rh-dex for 30 s. Finally, the eggs were washed with ASW and imaged with two channels of a confocal microscope (using rhodamine and fluorescein optics). We observed large red (Rh-dex) and green (Fl-dex) subcortical bodies which were interdispersed but not colocalized.

Our observation of cortical granule contents inside the lumina of the large transparent subcortical vesicles in activated UV-irradiated eggs, and the observation that dextrans labeled with different fluorescent markers segregate into different large subcortical vesicle populations when the dyes were applied extracellularly in sequential pulses argues that the endocytosis responsible for the net retrieval of 6% of an egg's volume is not mediated by small clathrin-coated vesicles. Consistent with this result is the finding that treating eggs with the protein kinase C activator PMA (200 nM) for 60 min triggered little uptake of Rh-dex (4.0 ± 0.9% of A23187 control, mean ± SEM, $n$ = 3). Activation of protein kinase C by PMA is known to trigger the formation of clathrin-coated vesicles in unfertilized sea urchin eggs without stimulating exocytosis (14).

### *Membrane Retrieval Is Inhibited by Procaine*

Little is known about the membrane intermediates involved in the mechanism of the direct bulk membrane retrieval that we have observed. Amphipathic membrane active compounds are known to inhibit membrane fusion reactions such as exocytosis, viral fusion, and fusion reactions involved in intracellular trafficking (13). For exocytosis they inhibit at a mechanistic step after calcium activation (55). Thus, while it has not been shown that these compounds inhibit endocytosis, we might expect that these compounds should inhibit calcium-triggered endocytosis, even after exocytosis has been completed, if calcium-triggered exocytosis and endocytosis share a common lipidic intermediate. We treated eggs with the amphipathic membrane active drug procaine (10 mM). A 5-min exposure to 10 mM procaine was sufficient to fully inhibit exocytosis in >95% of eggs. 5 min after treatment with procaine, eggs were activated with 50 μM A23187 in the presence of 100 μM Rh-dex. Over a 15-min period, procaine-treated eggs internalized only 3.5 ± 3.4% of the volume internalized by A23187-activated controls (mean ± SEM, $n$ = 5). When activated eggs were transferred into ASW containing 10 mM procaine after cortical granule exocytosis had been completed (5 min after the addition of A23187), dye uptake ceased abruptly ($n$ = 3). Thus procaine can inhibit rapid membrane retrieval by a mechanism other than inhibiting exocytosis (25), and suggests that curved fusion intermediates, such as stalks (12, 33, 59), might also be involved in membrane retrieval.

## *Discussion*

In many cell types exocytosis is often followed by endocytosis (4, 24, 29, 38, 40, 51). Studies in neurons (56), pituitary nerve terminals (42), and melanotrophs (52) based on electrical measurements suggest that after triggered exocytosis, large structures rapidly pinch off from the plasma membrane. Unfortunately, capacitance measurements alone do not discriminate between changes in membrane surface area due to endocytosis, from those caused by blebbing of the plasma membrane (2). Sea urchin eggs normally show little exocytotic or endocytotic activity before fertilization (9, 20, 21). Fertilization activates the egg from its state of dormancy into a rapidly growing and dividing cell. One of the many processes initiated at fertiliza-

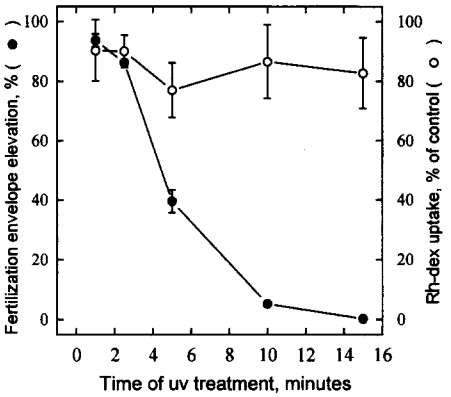


*Figure 8.* The effects of 254 nm UV light on fertilization envelope elevation and Rh-dex uptake. Eggs were treated with 254 nm UV light and activated with 50 μM A23187. Over a 15-min period fertilization envelope elevation as visualized using bright field microscopy (●) was progressively inhibited. In these same eggs Rh-dex uptake (○) was measured and was unaffected by UV light treatment.

tion is membrane trafficking, making this cell ideal for studying the relationship between exocytosis and endocytosis. Cortical granule exocytosis is the first and most obvious membrane fusion event following sperm–egg fusion. Later exocytotic events are involved in the deposition of components of the extracellular matrix (1, 6) and epithelial invagination (30). After each of these membrane fusion events, the embryo presumably compensates for the membrane added to its plasma membrane during exocytosis. Little is known about how this is accomplished.

After fertilization of eggs bathed with ASW containing fluorescent aqueous dyes or lipid-soluble dyes, there was a rapid increase of punctate fluorescence in subcortical regions of the eggs. This fluorescence sweeps across the egg as a wave that appears similar to the calcium wave that precedes it (49). New fluorescent structures were seen to form in less than a second. The size and density of these fluorescent structures, as well as the speed of their formation, are consistent with them being a manifestation of cortical granule exocytosis, since cortical granules can fuse within 15 ms of being exposed to calcium (54) and disperse their contents within 35 ms (35). By simultaneously imaging cortical granules and FM 1-43 fluorescence, the appearance of these fluorescent structures were correlated to within 0.5 s with the disappearance of granules (see also 50). In an egg bathed with a lipid-soluble fluorescent dye we showed that when a cortical granule disappears as visualized with DIC microscopy, there is the concomitant appearance of a fluorescent ring (Fig. 4). Presumably, upon fusion with the plasma membrane, the cortical granules protein contents are discharged and the fluorescent dyes diffuse through the newly formed fusion pores into the lumina of the granules. Measured using either aqueous- or lipid-phase fluorescent dyes, a number of these structures appeared to detach from the plasma membrane of the egg, since they could not be washed away by bathing with dye-free ASW. These vesicles no longer had extracellular continuity and thus are endosomes (57). Activation of eggs in ASW containing both aqueous- and lipid-phase fluorescent dyes (Fig. 5) demonstrated that both markers labeled the same structures. The variability observed in the amounts of each dye associated with any specific vesicle is thought to arise from vesicles which pinched off from the plasma membrane during dye perfusion. Dyes with different labeling kinetics would be present at different ratios if they had not reached equilibrium at the instant of endosome detachment. A subcortical vesicle of the size and abundance of the labeled endosomes was observed by electron microscopy in activated eggs (Fig. 1). These clear vesicles appeared to replace the fused cortical granules, and in UV-treated eggs often retained fragments of cortical granule contents (Fig. 9) suggesting that their membranes might be in part derived from the membranes of cortical granules. These large, clear subcortical vesicles might be

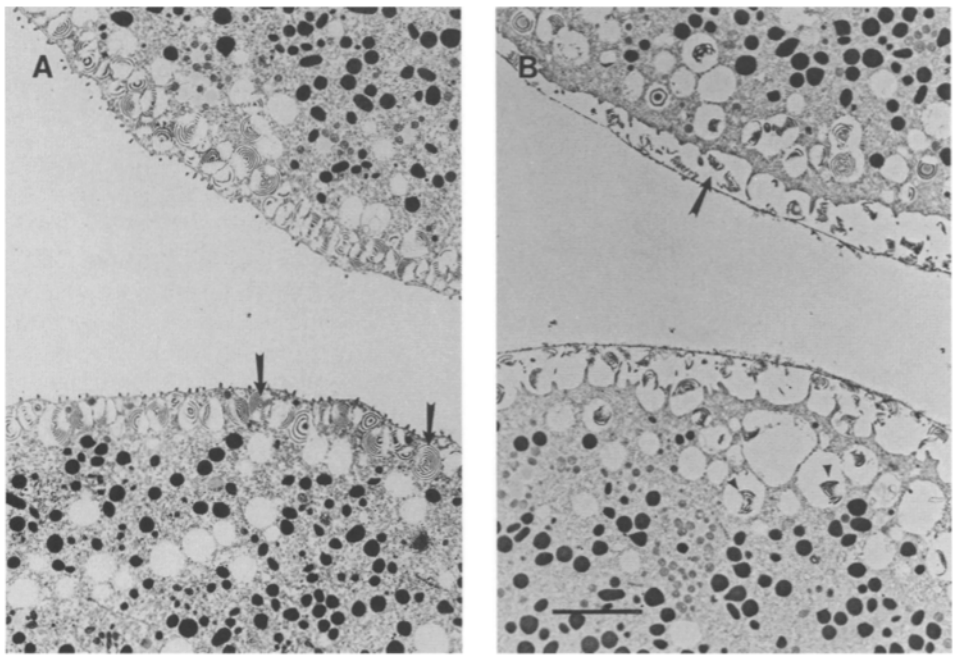


*Figure 9.* Electron micrographs of 254-nm UV light-treated eggs before and after activation. Eggs were treated with 254 nm UV light for 15 min. (*A*) In unfertilized eggs the cortical granules (indicated with arrows) remain intact and are associated with the plasma membrane. After activation with 50 μM A23187, UV-treated eggs (*B*) have undergone cortical granule exocytosis but granule cores have failed to disperse. Many semi-intact granule cores are trapped between the plasma membrane and the vitelline membrane (an example is indicated by the arrow). Semi-intact granule cores are also found in otherwise empty cortical vacuoles (*arrowheads*). The vesicles containing these cores could not have been formed solely by the fusion of small endocytotic vesicles. Bar, 5 μm.

related to acidic vesicles (31, 45) that apparently contain peroxidase activity (20), and may also have dynaminlike immunoreactivity (18). It is of some interest that cortical granules also contain ovoperoxidase (17) and dynaminlike immunoreactivity (18) suggesting that some components of the large clear vesicles are derived from cortical granules.

Using a dye uptake assay in populations of eggs we were able to define the kinetics of endocytosis after exocytosis. Approximately 30 s after egg activation endocytosis began and persisted over the next 15 min. Uptake was most rapid between three and five minutes after activation. The kinetics and amount of dye uptake were indistinguishable in eggs activated by fertilization or the $Ca^{2+}$ ionophore A23187. Over this 15-min period ~6% of the egg's volume was internalized.

We wanted to define how these large endosomes were formed after exocytosis in sea urchin eggs. Was it through a mechanism in which clathrin-coated pits were formed followed by pinching off of coated vesicles from the plasma membrane and subsequent fusion to form 1.5-μm-diam endosomes? Alternatively, did large endosomes directly form at the plasma membrane? A consideration of the quantitative data we obtained from the dye uptake assay in populations of eggs would suggest that the latter is most likely. To account for the volume of solute internalized through 0.1-μm-diam clathrin-coated vesicles would require the uptake of 15 times the area of membrane inserted during cortical granule exocytosis. Obviously, if the endocytosed vesicles were approximately the size of the exocytotic granules, the amount of membrane internalized during endocytosis would closely resemble that inserted during exocytosis. We tested this by giving pulses of two fluorescent dextrans and determining the subcellular fate of each. We found virtually no mixing of the two dyes when given 1 min apart. This exclusive localization suggests that the endosomes formed directly rather than through the concerted fusion of many smaller vesicles. However, this interpretation of the data relies on the premise that coated vesicles that form 1 min apart would fuse to the same early endosomal compartment. A confirmation of the direct formation of large endocytotic structures came from the finding that UV light prevented the dispersion of cortical granule protein cores after exocytosis. While it is possible that short wavelength UV light inhibits fertilization envelope elevation nonspecifically by randomly damaging cellular components, this is unlikely because UV-irradiated eggs go on to divide and form blastulae (48). UV light has been shown to induce dityrosine formation in proteins (32). The formation of dityrosines, catalyzed by a cortical granule peroxidase, is thought to stabilize the fertilization envelope after cortical granule exocytosis (23, 27). The treatment of unfertilized eggs with short wavelength UV light possibly leads to premature dityrosine formation and thus cross-linking of the granule contents, preventing them from expanding upon exocytotic membrane fusion (10). The observation that in UV-treated eggs, 1-μm-diam granule cores appear in large, otherwise empty cortical vacuoles suggests that after exocytosis, plasma membrane homeostasis is achieved through the direct retrieval of large endocytotic vesicles. In keeping with this, we found that treatment with the protein kinase C activator, PMA, which stimulates clathrin-dependent endocytosis in unfertilized eggs (14), failed to stimulate substantial dye uptake.

Subsequent to egg activation, endocytosis by clathrin-coated vesicles is triggered (9, 20, 21), probably via the activation of the protein kinase C pathway (14). This membrane retrieval pathway might allow the embryo to selectively regulate the lipid and protein composition of the plasma membrane in preparation for the development of a new organism. We have presented compelling evidence that the mechanism by which most of the membrane is retrieved after triggered exocytosis in sea urchin eggs involves the direct formation of large vesicles at the plasma membrane. To our knowledge, this is the first direct demonstration of the retrieval of membrane into large vesicular structures after triggered exocytosis in a living cell using noninvasive techniques. What we do not know is whether these endocytotic vesicles represent cortical granules that have fused with the plasma membrane, released their contents, and resealed or whether they are composed of a mosaic of plasma membrane and cortical granule membrane. The vesicles that pinch off into the cytoplasm (1.5 μm) are larger than those that fused during exocytosis (1.3 μm), as are the fluorescent rings observed during granule exocytosis (see Fig. 4). This is consistent with the transfer of plasma membrane through a fusion pore to exocytotic granules observed during flicker fusion in mast cells (37), and may allow for the retrieval or recycling (8) of specific plasma membrane components such as proteins that are no longer needed in a new embryo, for instance, sperm receptors (22). The lifetimes of fusion pores during flicker fusion are only of the order of hundreds of milliseconds to several seconds (36, 59), whereas we see membrane retrieval over a 15-min period. Thus, if cortical granules do transiently fuse with the plasma membrane, their dwell time in the plasma membrane must be much longer. Another difference between flicker fusion and the cortical granule exocytosis–membrane retrieval we have observed involves the apparent fusion pore diameter. When a flicker fusion pore expands beyond a diameter of ~36 nm, it has not been observed to close (16, 36). In UV-treated eggs, we know that some fusion pores must expand to a size which allows the release of the semi-intact granule core (~1 μm). In these eggs we still see an endocytotic response indistinguishable from nontreated eggs. These data argue that the large vesicles which form after triggered exocytosis are not the result of simply resealing a small diameter cortical granule fusion pore, but rather by the retrieval of membrane after fusion pores has fully dilated. Membrane retrieval is completed when large membrane invaginations pinch off from the plasma membrane to form large vesicles by a mechanism which is procaine sensitive, but remains to be elucidated.

We thank Joshua Zimmerberg, Michael Whitaker, Paul Blank, and Alex Sokoloff for stimulating discussions. We acknowledge Joshua Zimmerberg for his continued support and advice while pursuing this project.

Received for publication 24 May 1995 and in revised form 18 August 1995.

*References*

1. Alliegro, M. C., and D. R. McClay. 1988. Storage and mobilization of extra-

cellular matrix proteins during sea urchin development. *Dev. Biol.* 125: 208–216.
2. Alvarez de Toledo, G., and J. M. Fernandez. 1988. The events leading to secretory granule fusion. *In* Cell Physiology of Blood. The Rockefeller University Press, New York. 334–344.
3. Alvarez de Toledo, G., R. Fernandez-Chacon, and J. M. Fernandez. 1993. Release of secretory products during transient vesicle fusion. *Nature (Lond.).* 363:554–558.
4. Baker, P. F., and D. E. Knight. 1981. Calcium control of exocytosis and endocytosis in bovine adrenal medullary cells. *Philos. Trans. R. Soc. Lond. B Biol. Sci.* 296:83–103.
5. Betz, W. J., and G. S. Bewick. 1992. Optical analysis of synaptic vesicle recycling at the frog neuromuscular junction. *Science (Wash. DC).* 255:200–203.
6. Bisgrove, B. W., M. E. Andrews, and R. A. Raff. 1991. Fibropellins, products of an EGF repeat-containing gene, form a unique extracellular matrix structure that surrounds the sea urchin embryo. *Dev. Biol.* 146:89–99.
7. Breckenridge, L. J., and W. Almers. 1987. Currents through the fusion pore that forms during exocytosis of a secretory vesicle. *Nature (Lond.).* 328: 814–817.
8. Brown, M. S., R. G. Anderson, and J. L. Goldstein. 1983. Recycling receptors: the round-trip itinerary of migrant membrane proteins. *Cell.* 32:663–667.
9. Chandler, D. E. 1991. Multiple intracellular signals coordinate structural dynamics in the sea urchin egg cortex at fertilization. *Journal of Electron Microscopy Technique.* 17:266–293.
10. Chandler, D. E., M. Whitaker, and J. Zimmerberg. 1989. High molecular weight polymers block cortical granule exocytosis in sea urchin eggs at the level of granule matrix disassembly. *J. Cell Biol.* 109:1269–1278.
11. Chen, M. S., R. A. Obar, C. C. Schroeder, T. W. Austin, C. A. Poodry, S. C. Wadsworth, and R. B. Vallee. 1991. Multiple forms of dynamin are encoded by shibire, a Drosophila gene involved in endocytosis. *Nature (Lond.).* 351:583–586.
12. Chernomordik, L. V., G. B. Melikyan, and Y. A. Chizmadzhev. 1987. Biomembrane fusion: a new concept derived from model studies using two interacting planar lipid bilayers. *Biochim. Biophys. Acta.* 906:309–352.
13. Chernomordik, L. V., S. S. Vogel, A. Sokoloff, H. O. Onaran, E. A. Leikina, and J. Zimmerberg. 1993. Lysolipids reversibly inhibit Ca(2+)-, GTP- and pH-dependent fusion of biological membranes. *FEBS Lett.* 318:71–76.
14. Ciapa, B., I. Crossley, and G. De Renzis. 1988. Structural modifications induced by TPA (12-*O*-tetradecanoyl phorbol-13-acetate) in sea urchin eggs. *Dev. Biol.* 128:142–149.
15. Crossley, I., T. Whalley, and M. Whitaker. 1991. Guanosine 5′-thiotriphosphate may stimulate phosphoinositide messenger production in sea urchin eggs by a different route than the fertilizing sperm. *Cell Regul.* 2: 121–133.
16. Curran, M. J., F. S. Cohen, D. E. Chandler, P. J. Munson, and J. Zimmerberg. 1993. Exocytotic fusion pores exhibit semi-stable states. *J. Membr. Biol.* 133:61–75.
17. Deits, T., M. Farrance, E. S. Kay, L. Medill, E. E. Turner, P. J. Weidman, and B. M. Shapiro. 1984. Purification and properties of ovoperoxidase, the enzyme responsible for hardening the fertilization membrane of the sea urchin egg. *J. Biol. Chem.* 259:13525–13533.
18. Faire, K., and E. M. Bonder. 1993. Sea urchin egg 100-kDa dynamin-related protein: identification of and localization to intracellular vesicles. *Dev. Biol.* 159:581–594.
19. Fernandez, J. M., E. Neher, and B. D. Gomperts. 1984. Capacitance measurements reveal stepwise fusion events in degranulating mast cells. *Nature (Lond.).* 312:453–455.
20. Fisher, G. W., and L. I. Rebhun. 1983. Sea urchin egg cortical granule exocytosis is followed by a burst of membrane retrieval via uptake into coated vesicles. *Dev. Biol.* 99:456–472.
21. Fisher, G. W., R. G. Summers, and L. I. Rebhun. 1985. Analysis of sea urchin egg cortical transformation in the absence of cortical granule exocytosis. *Dev. Biol.* 109:489–503.
22. Foltz, K. R., J. S. Partin, and W. J. Lennarz. 1993. Sea urchin egg receptor for sperm: sequence similarity of binding domain and hsp70. *Science (Wash. DC).* 259:1421–1425.
23. Hall, H. G. 1978. Hardening of the sea urchin fertilization envelope by peroxidase-catalyzed phenolic coupling of tyrosines. *Cell.* 15:343–355.
24. Heuser, J. E., and T. S. Reese. 1981. Structural changes after transmitter release at the frog neuromuscular junction. *J. Cell Biol.* 88:564–580.
25. Hylander, B. L., and R. G. Summers. 1981. The effect of local anesthetics and ammonia on cortical granule-plasma membrane attachment in the sea urchin egg. *Dev. Biol.* 86:1–11.
26. Jaffe, L. A., S. Hagiwara, and R. T. Kado. 1978. The time course of cortical vesicle fusion in sea urchin eggs observed as membrane capacitance changes. *Dev. Biol.* 67:243–248.
27. Kay, E. S., and B. M. Shapiro. 1987. Ovoperoxidase assembly into the sea urchin fertilization envelope and dityrosine crosslinking. *Dev. Biol.* 121: 325–334.
28. Kirchhausen, T., and S. C. Harrison. 1981. Protein organization in clathrin trimers. *Cell.* 23:755–761.
29. Kline, D., and J. Stewart-Savage. 1994. The timing of cortical granule fusion, content dispersal, and endocytosis during fertilization of the hamster egg: an electrophysiological and histochemical study. *Dev. Biol.* 162: 277–287.
30. Lane, M. C., M. A. Koehl, F. Wilt, and R. Keller. 1993. A role for regulated secretion of apical extracellular matrix during epithelial invagination in the sea urchin. *Development.* 117:1049–1060.
31. Lee, H. C., and D. Epel. 1983. Changes in intracellular acidic compartments in sea urchin eggs after activation. *Dev. Biol.* 98:446–454.
32. Malencik, D. A., and S. R. Anderson. 1987. Dityrosine formation in calmodulin. *Biochemistry.* 26:695–704.
33. Markin, V. S., M. M. Kozlov, and V. L. Borovjagin. 1984. On the theory of membrane fusion. The stalk mechanism. *Gen. Physiol. Biophys.* 3:361–377.
34. McCulloh, D. H. 1985. Cortical reaction of sea urchin eggs: rate of propagation and extent of exocytosis revealed by membrane capacitance. *Development.* 27:178.
35. Mohri, T., and Y. Hamaguchi. 1990. Quantitative analysis of the process and propagation of cortical granule breakdown in sea urchin eggs. *Cell Struct. Funct.* 15:309–315.
36. Monck, J. R., and J. M. Fernandez. 1992. The exocytotic fusion pore. *J. Cell Biol.* 119:1395–1404.
37. Monck, J. R., G. Alvarez de Toledo, and J. M. Fernandez. 1990. Tension in secretory granule membranes causes extensive membrane transfer through the exocytotic fusion pore. *Proc. Natl. Acad. Sci. USA.* 87:7804–7808.
38. Nagasawa, J., W. W. Douglas, and R. A. Schulz. 1971. Micropinocytotic origin of coated and smooth microvesicles (synaptic vesicles) in neurosecretory terminals of posterior pituitary glands demonstrated by incorporation of horseradish peroxidase. *Nature (Lond.).* 232:341–342.
39. Nordmann, J. J., and J. C. Artault. 1992. Membrane retrieval following exocytosis in isolated neurosecretory nerve endings. *Neuroscience.* 49: 201–207.
40. Nordmann, J. J., P. F. Baker, M. Ravazzola, and F. Malaisse-Lagae. 1974. Secretion-dependent uptake of extracellular fluid by the rat neurohypophysis. *Nature (Lond.).* 250:155–157.
41. Obar, R. A., C. A. Collins, J. A. Hammarback, H. S. Shpetner, and R. B. Vallee. 1990. Molecular cloning of the microtubule-associated mechanochemical enzyme dynamin reveals homology with a new family of GTP-binding proteins. *Nature (Lond.).* 347:256–261.
42. Rosenboom, H., and M. Lindau. 1994. Exo-endocytosis and closing of the fission pore during endocytosis in single pituitary nerve terminals internally perfused with high calcium concentrations. *Proc. Natl. Acad. Sci. USA.* 91:5267–5271.
43. Rothman, J. H., C. K. Raymond, T. Gilbert, P. J. O'Hara, and T. H. Stevens. 1990. A putative GTP binding protein homologous to interferon-inducible Mx proteins performs an essential function in yeast protein sorting. *Cell.* 61:1063–1074.
44. Ryan, T. A., H. Reuter, B. Wendland, F. E. Schweizer, R. W. Tsien, and S. J. Smith. 1993. The kinetics of synaptic vesicle recycling measured at single presynaptic boutons. *Neuron.* 11:713–724.
45. Sardet, C. 1984. The ultrastructure of the sea urchin egg cortex isolated before and after fertilization. *Dev. Biol.* 105:196–210.
46. Schroeder, T. E. 1979. Surface area change at fertilization: resorption of the mosaic membrane. *Dev. Biol.* 70:306–326.
47. Smythe, E., and G. Warren. 1991. The mechanism of receptor-mediated endocytosis. *Eur. J. Biochem.* 202:689–699.
48. Spikes, J. D. 1944. Membrane formation and cleavage in unilaterally irradiated sea urchin eggs. *J. Exp. Zool.* 146:89–99.
49. Swann, K., and M. Whitaker. 1986. The part played by inositol trisphosphate and calcium in the propagation of the fertilization wave in sea urchin eggs. *J. Cell Biol.* 103:2333–2342.
50. Terasaki, M. 1995. Visualization of exocytosis during sea urchin egg fertilization using confocal microscopy. *J. Cell Sci.* 108:2293–2300.
51. Thilo, L. 1985. Selective internalization of granule membrane after secretion in mast cells. *Proc. Natl. Acad. Sci. USA.* 82:1711–1715.
52. Thomas, P., A. K. Lee, J. G. Wong, and W. Almers. 1994. A triggered mechanism retrieves membrane in seconds after Ca(2+)-stimulated exocytosis in single pituitary cells. *J. Cell Biol.* 124:667–675.
53. Ungewickell, E., and D. Branton. 1981. Assembly units of clathrin coats. *Nature (Lond.).* 289:420–422.
54. Vogel, S. S., K. Delaney, and J. Zimmerberg. 1991. The sea urchin cortical reaction. A model system for studying the final steps of calcium-triggered vesicle fusion. *Ann. NY Acad. Sci.* 635:35–44.
55. Vogel, S. S., E. A. Leikina, and L. V. Chernomordik. 1993. Lysophosphatidylcholine reversibly arrests exocytosis and viral fusion at a stage between triggering and membrane merger. *J. Biol. Chem.* 268:25764–25768.
56. von Gersdorff, H., and G. Matthews. 1994. Dynamics of synaptic vesicle fusion and membrane retrieval in synaptic terminals. *Nature (Lond.).* 367: 735–739.
57. Watts, C., and M. Marsh. 1992. Endocytosis: what goes in and how? *J. Cell Sci.* 103:1–8.
58. Zimmerberg, J., M. Curran, F. S. Cohen, and M. Brodwick. 1987. Simultaneous electrical and optical measurements show that membrane fusion precedes secretory granule swelling during exocytosis of beige mouse mast cells. *Proc. Natl. Acad. Sci. USA.* 84:1585–1589.
59. Zimmerberg, J., S. S. Vogel, and L. V. Chernomordik. 1993. Mechanisms of membrane fusion. *Annu. Rev. Biophys. Biomol. Struct.* 22:433–466.